energies

Article

Geomechanical and Technical Aspects of Torpedo Blasting under Seismic and Rockburst Hazard Conditions in Legnica–Glogow Copper District Mines

Zbigniew Burtan [1,*], Jerzy Cieślik [1], Dariusz Chlebowski [1], Paweł Piasecki [2] and Krzysztof Gzik [2]

[1] Faculty of Civil Engineering and Resource Management, AGH University of Krakow, Mickiewicza 30 av, 30-059 Cracow, Poland; jerz@agh.edu.pl (J.C.); chlebo@agh.edu.pl (D.C.)
[2] KGHM Polska Miedź S.A., O/ZG Rudna, Henryka Dąbrowskiego 50 av, 59-100 Polkowice, Poland; pawel.piasecki@kghm.com (P.P.); krzysztof.gzik@kghm.com (K.G.)
* Correspondence: burtan@agh.edu.pl

Abstract: The dominant hazard in the Polish copper ore mining industry (LGCD mines—Legnica–Glogow Copper District) is the occurrence of mining tremors and rockbursts. One of the effective active methods of preventing this threat is torpedo blasting, which results in disturbing the structure of roof rocks. A change in the integrity of a roof, especially in the tremor-generating layer or in the contact between stiff rock layers, reduces the possibility of an elastic energy concentration and may also be a kind of stress concentrator, provoking the destruction of rocks. This article presents original solutions for determining the areas of rock mass within a mining area where it is advisable to conduct torpedo blasting, and the experience of blasting in the Rudna copper mine in the LGCD is described. The first part of this article presents the results and experiences of using torpedo blasting prevention in the LGCD mine conditions in the Rudna mine. Assuming that due to the stress of the rocks, torpedo blasting brings the greatest benefits in the areas of elastic energy concentration, the second part of this article presents the results of numerical modeling, on the basis of which the zones of elastic energy concentration in the form of total, shear and volume deformation were determined in the vicinity of mining activities for typical geological and mining conditions in the LGCD. The importance of methods for the verification of the proposed solutions based on the analysis of seismic activity and geophysical mechanisms of events' foci and seismo-acoustic emissions was also emphasized. The numerical simulations performed and conclusions from in situ observations allowed the formulation of general principles for the selection of torpedo blasting parameters.

Keywords: underground mining; rock mechanics; mining tremors; rockburst hazard; torpedo blasting; mining experience

check for updates

Citation: Burtan, Z.; Cieślik, J.; Chlebowski, D.; Piasecki, P.; Gzik, K. Geomechanical and Technical Aspects of Torpedo Blasting under Seismic and Rockburst Hazard Conditions in Legnica–Glogow Copper District Mines. *Energies* **2024**, *17*, 1174. https://doi.org/10.3390/en17051174

Academic Editor: Manoj Khandelwal

Received: 30 September 2023
Revised: 12 February 2024
Accepted: 16 February 2024
Published: 1 March 2024

Copyright: © 2024 by the authors. Licensee MDPI, Basel, Switzerland. This article is an open access article distributed under the terms and conditions of the Creative Commons Attribution (CC BY) license (https://creativecommons.org/licenses/by/4.0/).

1. Introduction

Major natural hazards in copper mining in Poland include rockbursts and fault movements. Most rockbursts and rock mass destressing events registered in the Legnica–Glogow Copper District (LGCD) (Figure 1) have been the consequence of high-energy events, whilst the current rockbursting hazard level is associated with mining-induced seismicity. The potential for high-energy tremors is an inherent feature of copper fields within the LGCD region, mostly due to the occurrence of burst-prone roof rock strata over the worked-out areas and periodic faulting movements; these impacts are further exacerbated due to current mining activities [1]. The analysis of seismic activity recorded in recent years in the LGCD mine region shows that the most seismically active is the Rudna mine (Figure 1) [1,2].

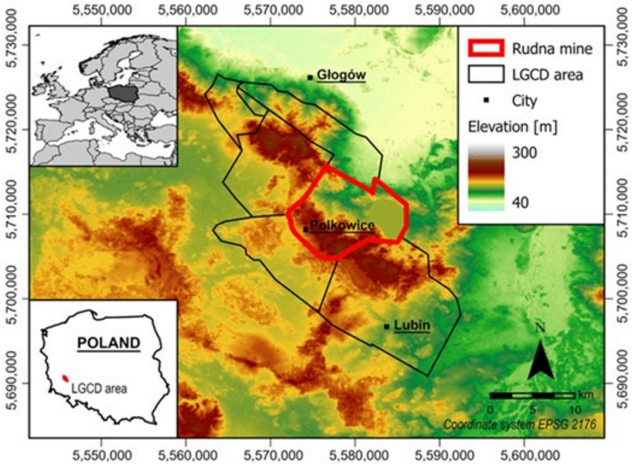

Figure 1. Location of the Rudna underground copper ore mine [3].

One of the effective active methods of preventing the threat of tremors and rockbursts is torpedo blasting performed in thick and highly stiff layers of the rock mass, which are the so-called tremor-prone layers. Torpedo blasting's aim is to provoke tremors or the local destruction of these layers (Figure 2) [4].

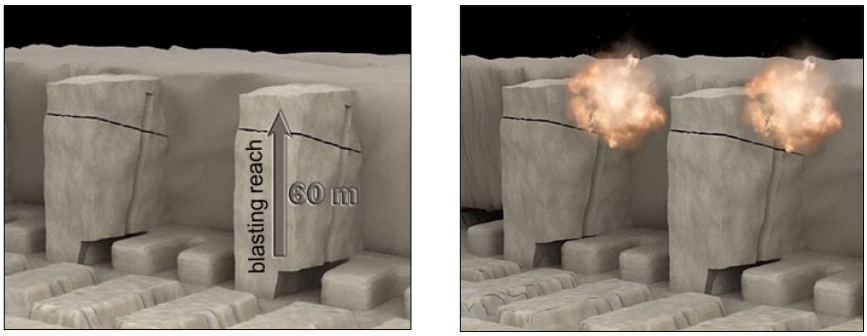

Figure 2. Scheme of torpedo blasting in a roof.

Considering the effect of torpedo blasting in terms of rockburst prevention, the effect of these blasts may be twofold, as follows [4]:

- Provoking a tremor, including a rockburst, as a result of disturbing the unstable stress balance of the rock mass.
- The creation of a local zone of destruction and weakening of the rock mass in the areas of expected stress concentration, without an immediate effect in the form of a tremor. Such a zone in the absorbing layer is a local place of stress concentration, which will result in the lower strength of the entire layer and the possibility of its destruction with the lower accumulation of elastic energy.

In the first case, the blasting should be characterized by a high intensity of paraseismic vibrations and should be adapted to the local mining and geological conditions due to possible difficulties in maintaining the working roof. It can then be combined with blasting in a larger number of exploitation workings to progress exploitation. In the second case, torpedo blasting may be an element of the so-called pre-emptive action for tremor prevention, planned and performed well in advance.

Torpedo blasting was used for the first time in Poland to reduce the risk of tremors and to ensure appropriate conditions for the collapse of roof rocks during the exploitation of coal seams in the Upper Silesian Coal Basin (USCB) [5]. Over time, these blastings became one of the elements of the active rockburst prevention system in the Polish coal mining industry (USCB mines) [5–10].

Torpedo blasting was also used in Polish copper mines in the LGCD [11,12], and as a result it was possible to exploit the deposit in rockburst-prone areas, in zones of geological anomalies [13], tectonic disturbances [14] and when operating in constrained conditions [12].

Blasting as a method of reducing the risk of rockbursts has been the subject of numerous international scientific works. Most of these works, however, are focused on stress relief blasts carried out at the working front or in the immediate roof in hard coal mines. Brauner [15–17] discussed the use of this method to limit rockbursts used in Germany.

The purpose of the destress blasting in seams or the roof and floor around the workings is to transfer the excessive induced stresses to the interior rock strata and to provide a protective barrier surrounding the excavation [16]. Kexin [18] and Xia et al. [19] demonstrated the application of the destress blasting to control of the floor heave in deep coal mines in China and reported a decrease in rock mass deformation after its application. Numerous publications have reported on stress relief blasting operations in Czech mines (part of USCB) [20–22]. Konicek et al. [23] highlighted the main benefits of using stress relief blasts as an effective method to overcome the high stresses causing rockbursts in these mines. In another article [24] by Konicek et al., the effectiveness of torpedo blasts in preventing rockbursts was estimated using the seismic effect method. Stress relief blasting has also been used in Indian coal mines [25], in South African ore mines [26] and in a Canadian copper mine [27,28]. Andrieux et al. [27] assessed the effectiveness of blasting using seismic tomography in one of the mines in Canada. Andrieux and Hadjigeorgiou [29] presented an empirical method of assessing the effectiveness of stress relief, based on various geotechnical and operational parameters. Fulawka et al. [30] proposed methods for assessing the effectiveness of stress relief blasts and also suggested innovative quantitative methods based on in situ seismic measurements. Modifications of stress relief blasting patterns aimed to improve their effectiveness in LGCD mines were presented by Mertuszka et al. [31]. The occurrence of high-stress zones determined by numerical calculations can be verified by a geophysical analysis of the mechanisms of foci events induced in these zones of tremors [32–34]. The widely used acoustic emission technology can also be used to monitor the destruction of roof rocks as a result of torpedo blasting [35,36], where the identification of seismo-acoustic signals allows for revealing the rock cracking mechanism.

The processes occurring within the rock strata as a result of stress relief blasting were also analyzed on the basis of numerical modeling. This type of analysis allows us to estimate the impacts of the blast energy depending on the sequence of blasts and the total amount of used explosives [30]. Numerical calculation techniques and their applications for analyzing the response of the rock strata to dynamic explosive load were proposed by Taylor et al. [37], who developed failure models capturing the characteristic dynamic fracture of rock under tension. Later, Maxwell and Young [38] developed numerical methods for examining objects under dynamic loads and simulated the extent of the failure zone under such loads.

Recently, numerical simulations have been used to describe the propagation of seismic waves in the rock mass after the detonation of explosives [39,40], and crack propagation around the blast hole [40–45]. Advanced simulations were also carried out to describe the initial destress of the rock mass after blasting [46–48]. Numerical methods were used to analyze the impact of blasting on underground infrastructure [49–52].

Geomechanical effects associated with large-scale rock mass destress were modeled by Vennes et al. [28,53]. The work of Miao et al. [54] reviewed contemporary methods of numerical modeling related to stress relief blasts.

The first part reported examples and case studies of torpedo blasting in LGCD conditions. The use of the rockburst prevention techniques was discussed recalling the blasting operations conducted in two sites within the Rudna mine, G-23/1 and G-11/8. In the first case, at the G-23/1 site, the torpedo blasting took place through long holes reaching high in the roof right to the contact zone between dolomite and anhydrite, in the region of the working face. In the second case, the torpedo holes were shorter and drilled near the edges of the mining site to be liquidated. These holes, blasted simultaneously with the blasting of

excavation faces, resulted in the division of a thick layer of strong dolomites into smaller ones, taking advantage of their natural cleavability. Interestingly, the torpedo blasting holes were located in the corner of the G-11/8 panel, where numerical calculations showed the highest concentration of elastic energy. In both cases, good blasting efficiency was achieved, confirmed by the occurrence of provoked tremors after an appropriate waiting period.

In consideration of the effectiveness of torpedo blasting in LGCD, it is extremely important to determine the region and zones within the rock mass that correspond to the highest elastic energy densities. These zones are determined by the parameters of the exploitation system and the geological structure of the deposit, i.e., the arrangement of geological layers (the occurrence of so-called tremor-prone layers) and the discontinuity of rock strata determining the conditions of contact between the layers, possible separation and slippage at the interface. These factors determining the effectiveness of torpedo blasting were the subject of numerical analyses undertaken in the second part of this study. The proposed methodology for determining highly stressed areas in the tremor-generating layer, with respect to torpedo blasting, is a simplified example of the use of geomechanical numerical modeling aimed at identifying tremor and rockburst hazard zones. It should be added that the first part of the study does not involve an in situ test following the numerical modeling procedure. Therefore, the continuation of the conducted research should be aimed at determining the areas, the scope and timing of stress relief blasting in order to improve the effectiveness of stress relief in the rock strata.

2. Case Study of Rudna Mine and the Use of Torpedo Blasting as Active Rockburst Prevention

Polish copper mines have already gained a great deal of experience in conducting active rockburst prevention. In the geological and mining conditions of the LGCD, a number of single or cyclic torpedo blasts would be carried out in the roof in order to disintegrate it, thus limiting the capability of the rock strata to accumulate elastic energy. Taking into account different lengths of boreholes, their location in relation to the tremor-prone layers and the parameters of the exploitation system, blasting tests were planned and carried out, among others, in the sites G-23/1, G-1/7, G-7/5, X/1 and G-11/8 in the Rudna mine [12]. The underlying assumptions were similar and focused on the use of explosive charges in the contact zone between the layers of limestone and anhydrite. This article provides a detailed report on two blasting operations (G-23/1, G-11/8) illustrating technical solutions for the local mining and geological conditions.

At the G-23/1 site, the deposit was formed by dolomites, copper-bearing shales and sandstones, and was located at a depth of ~1070 m, its thickness was 3.9–5.6 m and the average uniaxial compressive strength was approximately 60 MPa. The roof was made of compact dolomites, divided into slabs up to 1 m thick, the surfaces of which were covered with clay, gypsum and, less often, anhydrite. The thickness of the dolomite layer was approximately 60 m and its uniaxial compressive strength was approximately 102 MPa. On top of the dolomite, there was 143 m of anhydrite layers separated by dolomitic inclusions (9.7 m) and clay shales (4 m) (Figure 3).

After the rockburst that occurred in the final phase of exploitation of the G-23/1 panel, a single torpedoing of the roof was carried out as part of additional rockburst prevention, with four blast holes approx. 60 m (ϕ96 mm) in length, inclined at an angle of approx. 75 degrees to the horizontal. The holes were drilled from workings located along the front such that their ends reached the roof part of compact dolomites (Figure 4) and at the same time were found in a working area between 45 and 55 m of the working face (Figure 5). The total amount of emulsion explosives charge (emulgit 82 GP, cartridged) was ~1.0 Mg, which gave rise to a tremor with the energy rating of 8.6×10^3 J. However, the actual effect of the torpedo blasts is difficult to estimate because the blasts were carried out at the end of the exploitation, when it was practically coming to an end.

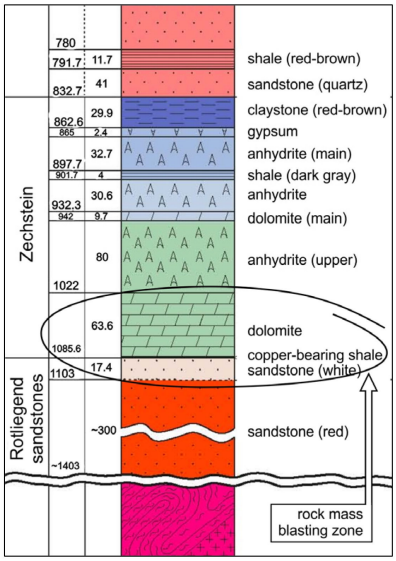

Figure 3. Lithological profile (part) of the deposit in the G-23/1 area.

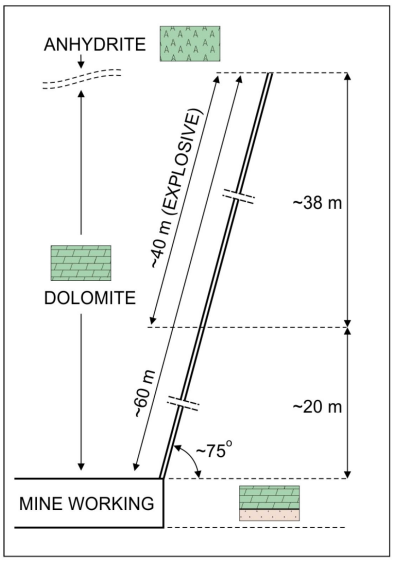

Figure 4. General scheme of torpedo blasting in the roof (G-23/1).

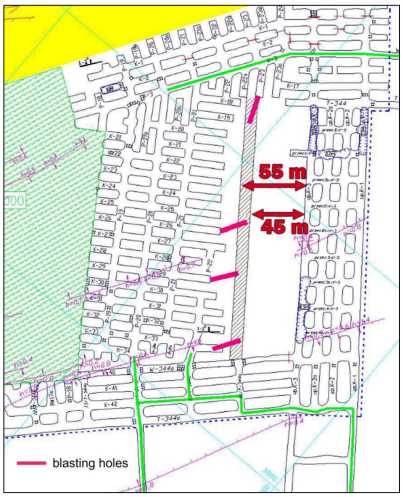

Figure 5. Sketch and location of blasts in the roof (G-23/1).

In the G-11/8 field, the deposit consisted of all lithological series, including dolomite, Zechstein shale and sandstone. The deposit was located at a depth of ~1125 m and its thickness was 2.5–3.1 m. The uniaxial compressive strength of the rock strata in the working face zone was around 78 MPa. In the roof of the workings, there was a dolomite layer approximately 15 m in thickness. These were cryptocrystalline dolomites, massive and compact, with a clear plate division (0.1–0.8 m), with the compressive strength of the order of 137 MPa. Directly overlying the dolomite formations, there was a 64 m layer of anhydrites, topped by rock salt (194 m), clay shales (1.5 m) and anhydrite again (48 m) (Figure 6).

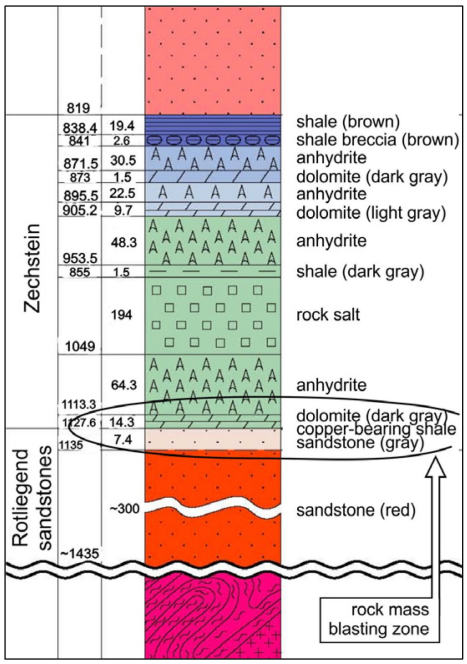

Figure 6. Lithological profile (part) of the deposit in the G-11/8 area.

After the rockburst, which destroyed a part of the workings, further mining activity in the area was carried out using an additional (non-routine) active prevention strategy, consisting of cyclical torpedo blasting in the roof (every 30 m of the face advance), simultaneously with group blasting in the face front. Blast holes with a length of ~15 m, ϕ45 mm reaching the roof section composed of carbonates (Figure 7), were drilled from workings located in the corner of the rear part of the working area (indicated with yellow color on the map in Figure 8) at an angle of approximately 70 degrees to the horizontal. In the period of 4 years from the resumption of mining activity, 20 torpedo blasting operations were carried out, consuming an average of 1.7 Mg explosive materials in each series, detonated only in the roof (not taking into account group blasting at the face front). Each blasting operation was performed using 60–80 blast holes, charged with emulsion explosives (emulgit RPT, in bulk) mechanically, in an amount of approximately 24 kg per hole. During the waiting period after the blasting works, a total of 42 rock mass tremors with energies above 10^3 J were recorded, including 17 events with energy ratings of the order of 10^5 J, 14 of the order of 10^4 J and 11 of the order of 10^3 J, respectively.

Based on the expertise gained during torpedo blasting at the Rudna mine, it should be stated [12] that drilling, loading and blasting ~60 m long holes in the roof (G-23/1, G-1/7) is feasible and well within the technical and organizational capabilities. Due to the relatively long period of implementation of blasting works, the continuous presence of miners in the area of the face front is required. This is a major security issue.

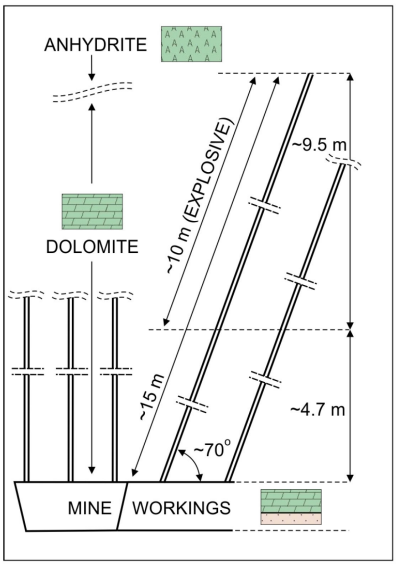

Figure 7. General scheme of torpedo blasting in the roof (G-11/8).

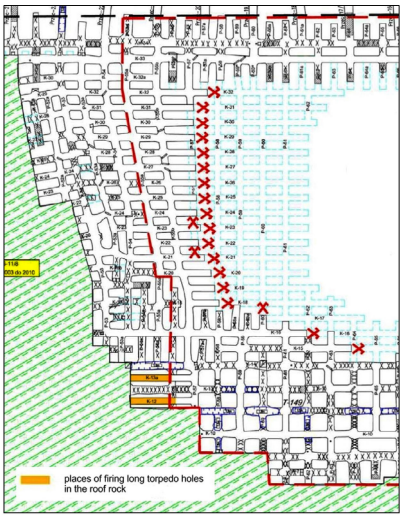

Figure 8. Sketch and location of blasts in the roof (G-11/8).

As a result of arranging the holes along the face front and mine working (e.g., in fields G-7/5, X/1) [12], portions of roof layers in the vicinity of the workings would be damaged, thus prompting the need to shut down these workings and disturbing the mining operations. In turn, blasting in the vicinity of a geological disturbance in the form of a syncline (section X/1) [12] allowed for stabilization of the convergence rate of mine workings in the working zone. Apparently, active prevention based on torpedo blasting is generally effective, yet further research and analyses (including the use of numerical tools) aimed at further improving its effectiveness are still fully merited.

3. Materials and Methods

Geomechanical Conditions for Torpedo Blasting—FEM Analysis

In the light of general assumptions regarding torpedo blasting, it is vital that the state of effort in the rock strata in the area to be mined should be known as well as the elastic strain energy accumulated in the rock strata, especially in the tremor-generating layers. The purpose of torpedo blasting is to induce a tremor by disturbing the state of stress equilibrium in the rock strata, where the failure is imminent. This is possible by supplying elastic energy that will provoke a tremor under given conditions. Assuming the

continuity of the rock strata and simplifying the site geometry, it is possible to determine the distribution of elastic strain energy and effort to identify regions where the use of torpedo blasting should be most effective.

Accordingly, 3D numerical FEM models were built emulating the general geological conditions and the room-pillar mining system of the LGCD and the G-23/1 and G-11/8 sites in the Rudna mine (Figure 1). Tremor-prone layers in these areas responsible for seismic activity are represented by dolomitic limestone and anhydrites of variable thicknesses (Table 1 and Figure 9).

Table 1. Parameters of rock layers in the Rudna mine used in the numerical analyses.

Rock Layer	Thickness [m]	E_m [GPa]	ν [-]
Anhydrite	100	17.9	0.22
Dolomite	40	13.3	0.22
Dolomite deposit	4.5	8.8	0.24
Sandstone	100	5.7	0.35
Liquidation	4.5	0.2	0.4

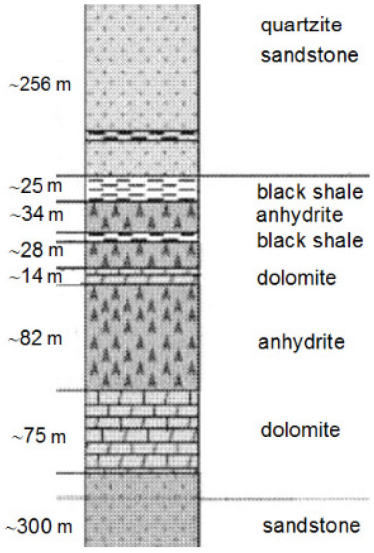

Figure 9. Example of the geological profile of the Rudna mine.

The geometry of the numerical model, the FEM mesh and the boundary conditions are shown in Figure 4. The calculations were performed on a linear-elastic constitutive model of the rock strata, whose parameters were determined on the basis of geological data from Rudna mine and recalling the Hoeck–Brown relationship [55]. Underlying the model are the general assumptions of the room and pillar exploitation system used in the LGCD, i.e., the front section, working area (Figure 10b—red), the mining liquidation zone (Figure 10b—green) and the abandoned liquidation zone (Figure 10b—grey) These aspects were incorporated by adopting equivalent deformation parameters of the corresponding spaces. In this approach, small operational pillars were not modeled. The conditions assumed in the adopted FEM calculations in terms of site geometry correspond to the mining operations in the G-23/1 and G-11/8 sections of the Rudna mine (Figure 10a).

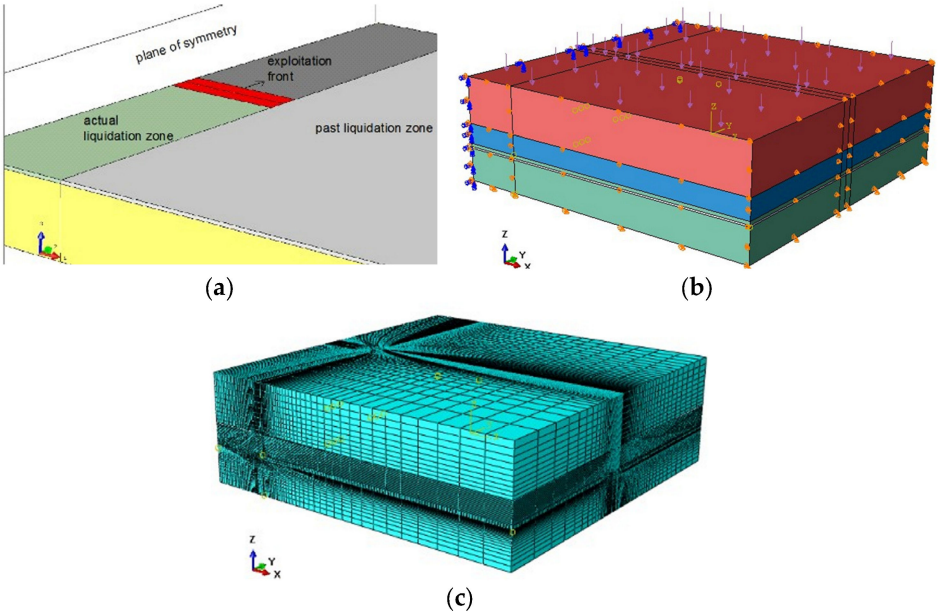

Figure 10. The computational model assumptions, (**a**) geometry, (**b**) boundary conditions, (**c**) FEM mesh.

The proposed method of analysis is a simplified one and the numerical procedure was applied without handling each and every variant of the room-pillar working system used in the LGCD. This simplification strategy yields only the results of analyses that are adequate to typical mining situations encountered in LGCD conditions. A solution was adopted whereby separate pillars should be replaced by zones with equivalent elastic parameters, whose impacts on the high roof layers are similar to those exerted by separate pillars. These parameters were adopted on the basis of previous calculations and recalling the authors' expertise in modeling typical convergences measured in the mine working area. Obviously, advanced calculations could and should take into account the modeling of separate pillars, as discussed in [56,57].

The calculation procedure relies on the displacement boundary conditions of the model corresponding to zero displacements on the respective edges of the model (Figure 10b). The acting load was the vertical normal stress exerted on the upper horizontal edge of the model corresponding to the mining depth of 1100 m. The problem was solved in a multi-step computational procedure reflecting the conditions of the initial state of stress and the progress of mining operations. The problem was treated as geometrically non-linear; therefore, the FEM equations in the ABAQUS v.6.12 computing system were solved using the Newton–Raphson incremental iterative procedure.

4. Results and Discussion—Rock Mass Effort and Elastic Strain Energy as Factors Determining the Effectiveness of Torpedo Blasting

4.1. The Effort of the Tremor-Prone Layer in the Working Area

In the context of effectiveness of torpedo blasting, two aspects are of primary importance, i.e., the direction of the blast holes and the size of the explosive. These two factors are related to the geological and mining conditions, but they can be determined using the analysis of effort and distribution of elastic energy accumulated in the rock strata.

The dynamic stresses necessary to trigger a tremor can be determined by Expression (1) resulting from the Mohr–Coulomb failure criterion (Figure 11).

$$\sigma_d(x,y,z) \geq W_{M-C} - W_S(x,y,z) \quad (1)$$

where

W_{M-C}—a measure of critical effort according to the Mohr–Coulomb M-C criterion;
$W_{M-C} = 2c\cos\varphi + (\sigma_1 + \sigma_3)\sin\varphi$;

$W_S(x, y, z)$—a measure of effort due to static stress tensor (before blasting);
$W_S(x, y, z) = \sigma_1 - \sigma_3$;
$\sigma_d(x, y, z)$—a effort required to trigger a tremor under the dynamic load caused by torpedo blasting;
σ_1, σ_3—greatest and least principal stress.

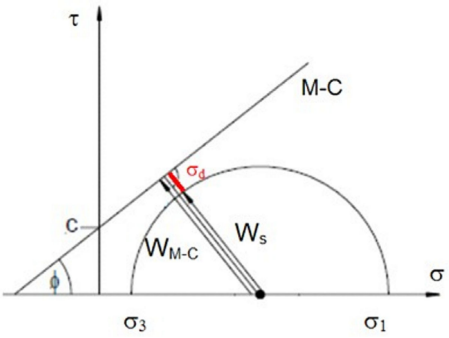

Figure 11. Mohr–Coulomb failure envelope. The effort needed to trigger tremors is marked in red.

Expression (1) applies only to regions within the rock strata where the effort W is defined as:

$$W = \frac{W_S}{W_{M-C}} \tag{2}$$

taking the value $W < 1$. According to the authors, the regions of the rock strata where the effort value falls in the range of $0.8 < W < 1$ can be considered the most favorable in the context of locating blast holes, because the value of dynamic stresses σ_d required to fracture the rock strata there is relatively small. The map of the strain factor W (2) covering the rock strata in the dolomitic limestone layer treated as a tremor-prone layer in LGCD conditions is shown in Figure 12a.

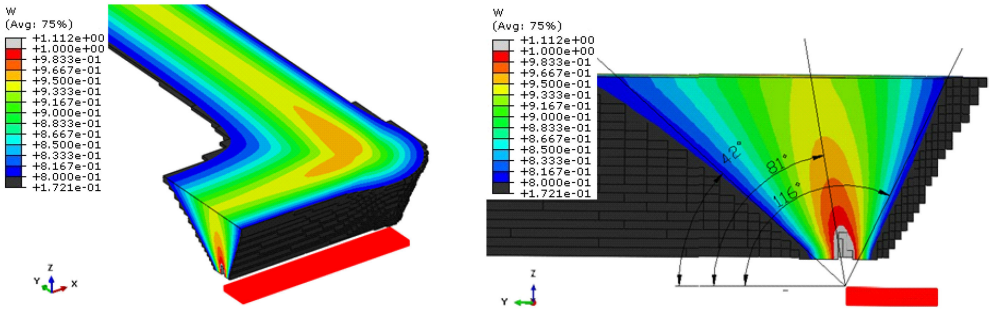

Figure 12. Effort map in the dolomitic limestone layer for the Rudna mine conditions. (**a**) Perspective view, (**b**) cross section view.

In the tremor-prone layer, the area with the effort value of $0.8 < W < 1$ is found in front of the excavation and is wedge- shaped with a wall inclination of 42–116 degrees. The highest effort value in the analyzed layer is registered at an angle of 81 degrees to the horizontal, towards the working zone (Figure 12b). In the corner of the working zone (Figure 12a), the high effort section is locally wider. Drilling holes for torpedo blasting in the indicated range should prove most effective in the context of triggering tremors. In addition, torpedo holes in this region are a good choice as they enhance the effect of additional discontinuity between the layers. Damaging the natural contact between the tremor-prone layer and the surrounding strata in this area should be the most effective.

4.2. Analysis of the Distribution of Elastic Strain Energy in the Vicinity of the Working Zone

Underlying the analyses of the elastic energy distribution in the vicinity of the working zone was the model in which limestone, anhydrite and dolomite layers were able to slip against each other, in accordance with Coulomb's friction law with a friction coefficient of $\mu = 0.6$.

The calculation results were presented in the form of maps of the distribution of elastic strain energy density coefficients: k_{Ac}—total, k_{Af}—shear strain and k_{Av}—volumetric strain elastic energy, defined as follows:

$$A_c = \frac{1}{2E}\left[\sigma_x^2 + \sigma_y^2 + \sigma_z^2 - 2\nu\left(\sigma_x\sigma_y + \sigma_y\sigma_z + \sigma_z\sigma_x\right) + 2(1+\nu)\left(\tau_{xy}^2 + \tau_{zx}^2 + \tau_{yz}^2\right)\right] \quad (3)$$

$$A_f = \frac{1+\nu}{6E}\left[\left(\sigma_x - \sigma_y\right)^2 + \left(\sigma_y - \sigma_z\right)^2 + \left(\sigma_z - \sigma_x\right)^2 + 6\left(\tau_{xy}^2 + \tau_{zx}^2 + \tau_{yz}^2\right)\right] \quad (4)$$

$$A_v = \frac{1-2\nu}{6E}\left(\sigma_x + \sigma_y + \sigma_z\right)^2 \quad (5)$$

$$k_{Ac} = \frac{A_c}{A_c^p};\ k_{Af} = \frac{A_f}{A_f^p};\ k_{Av} = \frac{A_v}{A_v^p} \quad (6)$$

where

A_c—density of total elastic energy; A_f—density of shear strain elastic energy; A_v—density of volumetric strain elastic energy; the index p indicates the values of initial energy corresponding to the initial state of stress.

The spatial distributions of the elastic strain energy density coefficients around the working zone are illustrated in Figure 13.

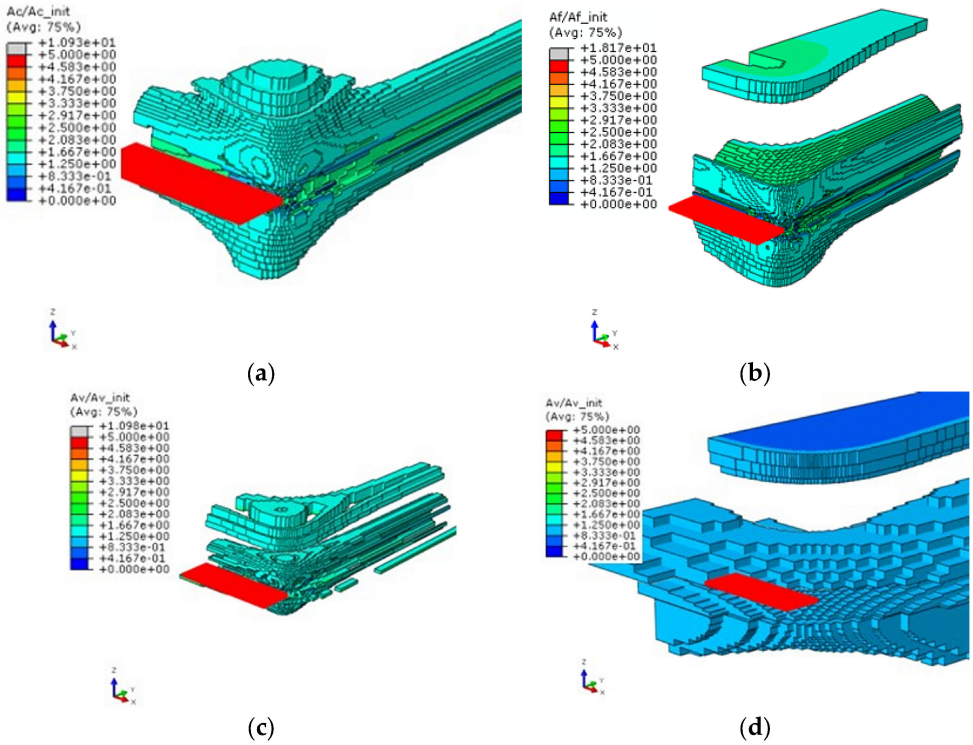

Figure 13. Volumes of rock around the working zone corresponding to the values of the elastic energy density coefficients in the roof layers: (**a**) Total $1.5 < k_{Ac} < 1.7$; (**b**) shear $1.5 < k_{Af} < 1.7$; (**c**) volumetric $1.5 < k_{Av} < 1.7$ and (**d**) volumetric $k_{Av} < 1$.

Maps of the total elastic energy coefficient in the cross-sections perpendicular to the face front are shown in Figure 14a, for various distances from the corner of the front section and in cross-sections parallel to the front section in Figure 14b.

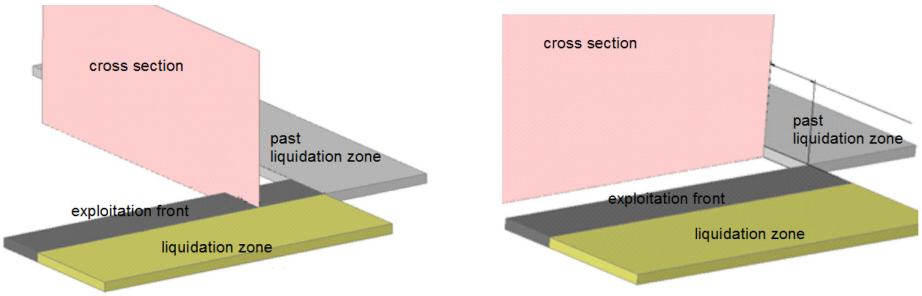

(**a**) (**b**)

Figure 14. Cross-sections perpendicular (**a**) and parallel (**b**) to the working face, showing elastic energy density maps.

First, Figure 9 shows maps of three types of energy density in the cross-section perpendicular to the working front (Figure 14a), in the middle of the working front section.

It should be noted that extreme values of individual energy concentration coefficients occur in the front of working zone and in the roof in the dolomitic limestone layer (tremor-prone layer) ahead of the front section. Ahead of the working front, there is an increase in the concentration of strain energy k_{Af} (Figure 15b) in the floor and roof of the limestone layer, the maximum of which is located approximately 40 m in front of the working zone. Above the working space, the load acting on the roof layers is relieved, which is accompanied by a decrease in the value of the volume strain energy density, which goes down below $k_{Av} < 1$ (Figure 15c). This is important in the context of the stress analysis in the roof layers in this region, because with a small value of the stress axiator, a smaller value of the stress deviator is also required to trigger the rock failure. A good indicator of energy concentration in the rock strata is the total energy elastic density coefficient k_{Ac} (Figure 15a), which comprehensively illustrates the accumulation of individual types of strain elastic energy. Therefore, further analysis of elastic energy distributions around the entire working zone, in individual sections perpendicular and parallel to the working front (Figure 13a,b), was conducted basing on the total elastic energy density coefficient k_{Ac} (Figure 16).

The distributions of the total strain energy density coefficient values k_{Ac} for cross-sections parallel to the working front are shown in Figure 17.

Additionally, calculations were performed for this variant of the model in which slippage between the tremor-prone layer and the surrounding rocks would be precluded. The results of the numerical simulations performed for both variants: that precluding slippage between the layers (Figure 18a) and that admitting slippage (Figure 18b) yield the spatial distribution of the total energy density coefficient k_{Ac}. In regard to the symmetry of the working zone, the drawing covers half of the area of the modeled exploitation site.

Obviously, the extreme values of total elastic energy coefficient k_{Ac} are registered in the roof strata in the vicinity of the working front, in the direction inclined to the horizontal at an angle of 63–69°. In the corner of the site, the value of total elastic strain energy is the highest and decreases over a distance of approximately 90 m, as we move away towards the runway and the center part of the working front.

These analyses reveal that concentrations of the strain energy density coefficient k_{Af} occur in regions located in front of the working front (Figure 15b). The total energy concentration k_{Ac} also corresponds to this situation (Figures 15 and 16). This is consistent with observations and analyses of the occurrence of tremor epicenters, the largest number of which occur in front of the working front at a distance of less than 50 m [58,59]. As regards the potential of high-energy tremor occurrence, the most unfavorable conditions prevail when there is a large accumulation of shear strain energy in a given region. In such situations, seismicity analyses should allow for the possibility of correlating the mechanism

of rock failure through shearing with the geophysical mechanism of the tremor focus, in which the shear component plays a dominant role [33,34].

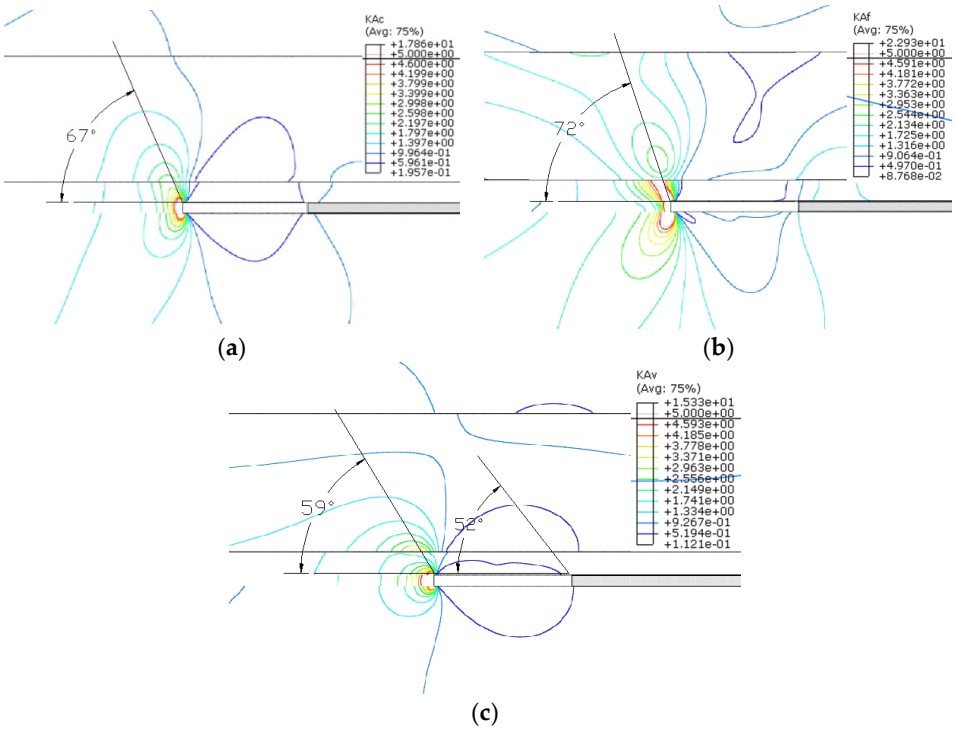

Figure 15. Map of strain energy coefficients in roof layers. (**a**) k_{Ac} total, (**b**) k_{Af} shear and (**c**) k_{Av} volumetric. The location of extreme values is marked with straight lines.

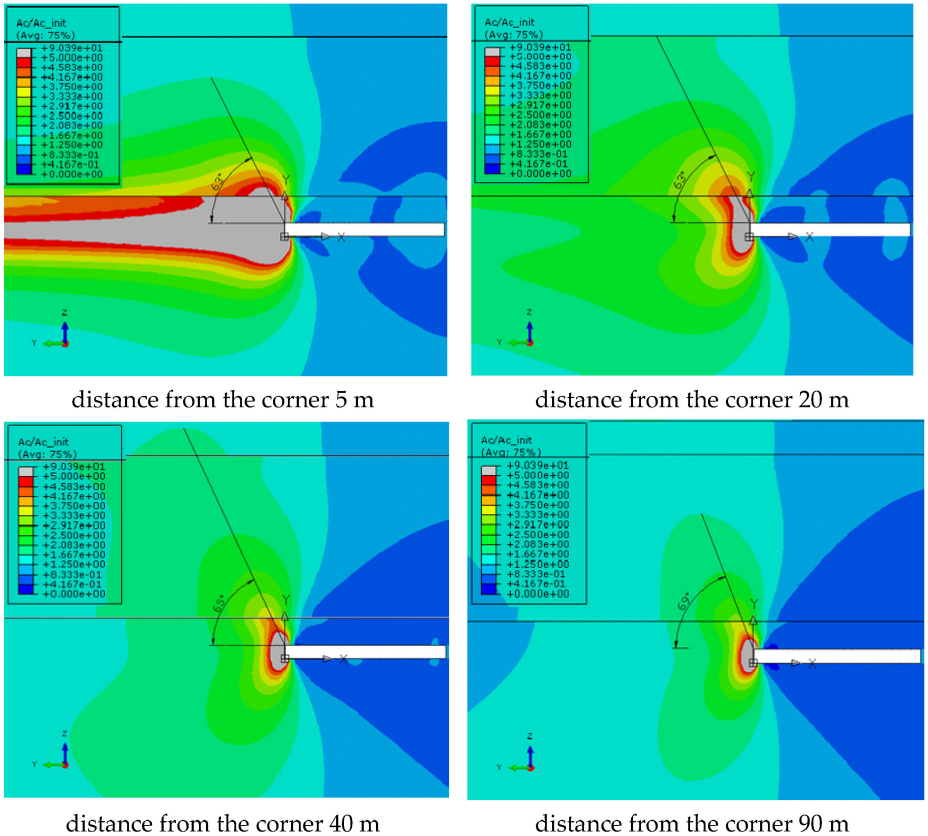

Figure 16. Maps of the total energy elastic density coefficient k_{Ac} in the cross-section perpendicular to the working front (Figure 14a).

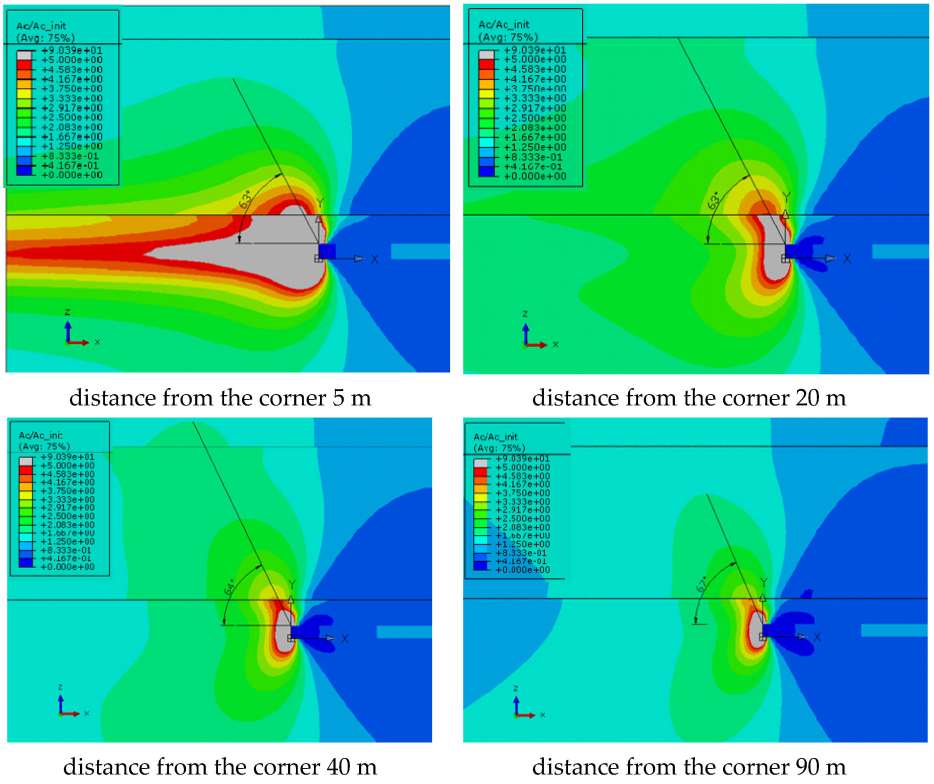

Figure 17. Maps of the total energy elastic density coefficient in the roof layers k_{Ac}, parallel to the working front (Figure 14b).

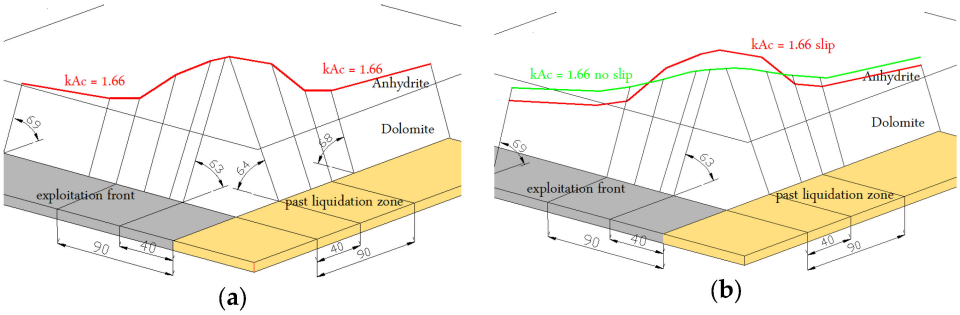

Figure 18. Spatial visualization of the distribution of the range of coefficient k_{Ac} with a value of 1.66 for models (**a**) with slippage between layers (**b**) without slippage.

Low values of the volume strain energy coefficient k_{Av} are registered in regions where low-energy tremors may potentially occur, such as the roof rock above the working zone and in the goafs (Figure 15c). These analyses lead us to the conclusion that coefficients of shear strain energy density k_{Af} and the density of total elastic energy k_{Ac} can be treated as measures of the potential risk of high-energy tremors of the rock strata, and the coefficients of volumetric strain energy density k_{Av} is associated with the regions of low-energy tremor occurrence.

5. Conclusions

The dominant hazard in the Polish copper mining industry (LGCD mines—Legnica-Glogow Copper District) is the occurrence of mining tremors and rockbursts. One of the effective active methods of preventing this hazard is torpedo blasting, which results in disturbing the structure of the roof rocks. These blastings should be considered with two effects in mind: the "triggering" a tremor and "weakening" of the rock strata.

Currently, torpedo blasting in the roof rock is still continued in the Rudna mine as a part of the rockburst prevention strategy. These are primarily cyclical blasts aimed at locally weakening the roof layers in the mining liquidation zones. They are performed to reduce the capability of roof rocks to accumulate large energies and, consequently, to provoke low-energy tremors.

Extensive research as well as practical experience acquired in the Rudna mine (LGCD) during blasting in compact roof layers lead us to the following conclusions:

- There are possibilities of active rockburst prevention in the torpedo blasting form based on long blast holes up to approx. 60 m long and it is not a problem from a technical point of view, although it is complicated in implementation,
- Sections of torpedo holes filled with explosive material should be located in zones with the maximum effort and accumulation of elastic energy (at present or in the future); in relation to the geomechanical conditions in the LGCD area, the blast holes should be inclined at an angle of approximately 65 ± 5 degrees,
- Blast holes should reach the contact zone between limestone and anhydrite; by changing the type of contact a weakening effect will be achieved and, consequently, a reduction in the value of the accumulated energy of elastic deformations; events caused by the cracking of the tremor-producing layer will be more frequent, but their seismic energies will be lower (which will result in a reduced risk of rockbursts),
- Torpedoing the roof has positive effects in the form of induced tremors, especially when used in the area of the edges of old goafs and in tectonic disturbance zones,
- The implementation of torpedo blasting may, however, lead to local destruction of roof layers in the immediate vicinity of active workings, thus disturbing the technological process of mining works.

Based on the numerical calculations performed, it can be concluded that appropriate geomechanical computer simulations, compared with analyses of geophysical mechanisms of tremor foci and with the results of monitoring of the level of roof failure by seismo-acoustic emission methods, may help identify the potential hazard areas. From the standpoint of active rockburst prevention in the form of torpedo blasting, these regions are considered to be areas where this type of prevention should be used.

This research work should be continued to determine the areas, scope and timing of stress relief blasting operations in order to improve the effectiveness of rock mass relaxation in conditions of high rockburst risk.

Author Contributions: Research/conceptualization of the paper, data analysis and verification, stress/energy state modelling, results comparison, conclusions, final editing, data collecting and preliminary analysis, results visualization, draft text editing, Z.B., J.C., D.C., P.P. and K.G. All authors have read and agreed to the published version of the manuscript.

Funding: The research was funded by AGH University of Krakow; subsidy numbers 16.16.100.215, 501.696.7996.

Data Availability Statement: Data is contained within the article.

Conflicts of Interest: Authors Paweł Piasecki and Krzysztof Gzik were employed by the company KGHM Polska Miedź S.A. The remaining authors declare that the research was conducted in the absence of any commercial or financial relationships that could be construed as a potential conflict of interest.

References

1. Burtan, Z. The influence of regional geological settings on the seismic hazard level in copper mines in the Legnica-Głogów Copper Belt Area (Poland). In Proceedings of the AG 2017-3rd International Conference on Applied Geophysics. E3S Web of Conferences, Gniew, Poland, 21–23 June 2017; Volume 24, p. 01004. [CrossRef]
2. Cieślik, J.; Burtan, Z.; Chlebowski, D.; Zorychta, A. Geomechanical analysis of location and conditions for mining-induced tremors in LGOM copper mines. *J. Sustain. Min.* **2017**, *16*, 94–103. [CrossRef]
3. Owczarz, K.; Blachowski, J. Application of DInSAR and Spatial Statistics Methods in Analysis of Surface Displacements Caused by Induced Tremors. *Appl. Sci.* **2020**, *10*, 7660. [CrossRef]

4. Zorychta, A.; Cieślik, J.; Burtan, Z.; Chlebowski, D. Geomechaniczne warunki poprawy efektywności strzelań torpedujących w kopalniach LGOM. *CUPRUM—Czas. Nauk.-Tech. Górnictwa Rud Miedzi* **2015**, *3*, 83–93. (In Polish)
5. Pawłowicz, K. *Strzelania Torpedujące Jako Metoda Zapobiegania Tąpaniom*; Prace Naukowe GiG; Główny Instytut Górnictwa: Katowice, Poland, 1996; Volume 803. (In Polish)
6. Krzyżowski, A. Rockburst prevention in hard coal mines (in Poland). In Proceedings of the 13th International Scientific-Technical Symposium ROCKBURSTS 2002, Ustron, Poland, 12–15 November 2002; Central Mining Institute in Katowice: Katowice, Poland, 2002; pp. 193–236.
7. Drzewiecki, J.; Kabiesz, J. Dynamic events in roof strata—Occurrence and prevention. *Coal Sci. Technol. Mag.* **2008**, *235*, 55–57.
8. Wojtecki, Ł.; Mendecki, M.J.; Zuberek, W.M. Determination of Destress Blasting Effectiveness Using Seismic Source Parameters. *Rock Mech. Rock Eng.* **2017**, *50*, 3233–3244. [CrossRef]
9. Wojtecki, Ł.; Konicek, P.; Schreiber, J. Effects of torpedo blasting on rockburst prevention during deep coal seam mining in the Upper Silesian Coal Basin. *J. Rock Mech. Geotech. Eng.* **2017**, *9*, 694–701. [CrossRef]
10. Olechowski, S.; Ćwiękała, M. Rock bursts prevention in conditions of increased seismic activity during the exploitation of seam 713/1-2 with wall II-E1 in KWK ROW Ruch Rydułtowy coal mine. *Przegląd Górniczy* **2021**, *10*, 26–33. (In Polish)
11. Butra, J. *Eksploatacja Złoża rud Miedzi w Warunkach Zagrożenia Tąpaniami i Zawałami*; KGHM Cuprum CBR: Wrocław, Poland, 2010. (In Polish)
12. Anderko, A.; Laskowski, M.; Mirek, A.; Osman, R.; Wróbel, J. Additional prevention against tremors with the use of blasting in roof layers—Tests of KGHM Polska Miedź S.A. Rudna copper ore mine. *Przegląd Górniczy* **2015**, *2*, 1–9. (In Polish)
13. Gzik, K.; Laskowski, M.; Wróbel, J. *Wpływ Strzelania Krawędziowego na Zachowanie Górotworu w Polu X/1 O/ZG Rudna, Prowadzonym w Szczególnie Trudnych Warunkach Geologiczno-Górniczych*; Górnicze Zagrożenia Naturalne—Praca Zbiorowa; Wydawnictwo GIG: Katowice, Poland, 2010. (In Polish)
14. Gzik, K.; Laskowski, M.; Świder, M.; Mirek, A. *Wpływ Uwarunkowań Tektonicznych na Prowadzenie Robót Eksploatacyjnych w Polu G-7/5 O/ZG Rudna*; Kabiesza, J., Ed.; Zagrożenia i Technologie—Praca Zbiorowa; Wydawnictwo GIG: Katowice, Poland, 2012. (In Polish)
15. Brauner, G. *Experiences with Destress Blasting Technique in Radbod Colliery*; Verlag Gluckauf GmbH: Essen, Germany, 1976; Volume 112, pp. 951–957. (In German)
16. Brãuner, G. *Rockbursts in Coal Mines and Their Prevention*; Balkema: Rotterdam, The Netherlands, 1994; 144p.
17. Velsen-Zerweck, R. *Destress Coal Blasting in Ruhr Hardcoal Mining in Rockburst Prevention*; Nobel Hefte; Sprengtechnischer Dienst der Orica Germany: Troisdorf, Germany, 1984; Volume 50, pp. 85–92. (In German)
18. Kexin, D. Maintenance of roadways in soft rock by roadway-rib destress blasting. *China Coal Soc.* **1995**, *20*, 311–316. (In Chinese)
19. Xia, H.; Xu, Y.; Zong, Q.; Fu, J. Research on the technology of unloading blast for a deep soft rock tunnel and its engineering application. *J. Anhui Univ. Sci. Technol. (Nat. Sci.)* **2007**, *27*, 13–16. (In Chinese)
20. Holecko, J.; Ptacek, J.; Takla, G.; Konecny, P. Rock bursts in the Czech part of the Upper Silesian Coal Basin—Features, theoretical models and conclusions for practice. In Proceedings of the 9th ISRM Congress, International Society for Rock Mechanics, Paris, France, 25–28 August 1999; pp. 1101–1104.
21. Dvorsky, P.; Konicek, P. Systems of rock blasting as a rockburst measure in the Czech part of Upper Silesian Coal Basin. In Proceedings of the 6th International Symposium on Rockburst and Seismicity in Mines, Perth, Australia, 9–11 March 2005; pp. 493–496.
22. Konicek, P.; Konecny, P.; Ptacek, J. Destress rock blasting as a rockburst control technique. In Proceedings of the 12th ISRM Congress, International Society for Rock Mechanics, Beijing, China, 18–21 October 2011; pp. 1221–1226.
23. Konicek, P.; Saharan, M.R.; Mitri, H. Destress Blasting in Coal Mining—State-of-the-Art Review. In Proceedings of the First International Symposium on Mine Safety Science and Engineering. Procedia Engineering, Beijing, China, 26–29 October 2011; Volume 26, pp. 179–194.
24. Konicek, P.; Soucek, K.; Stas, L.; Singh, R. Long-hole destress blasting for rockburst control during deep underground coal mining. *Int. J. Rock Mech. Min. Sci.* **2013**, *61*, 141–153. [CrossRef]
25. Chouhn, R.K.S. Induced seismicity of Indian coal mines. *Phys. Earth Planet. Inter.* **1986**, *44*, 82–86. [CrossRef]
26. Toper, A.Z.; Adams, D.J.; Janse Van Rensburg, A.L. The effects of preconditioning blast in confined rock. In Proceedings of the ISRM International Symposium on Integral Approaches to Applied Rock Mechanics, Santiago, Chile, 10–14 May 1994.
27. Andrieux, P.P.; Brummer, R.K.; Liu, Q.; Simser, B.P.; Mortazavi, A. Large-scale panel destress blast at Brunswick Mine. *CIM Bull.* **2003**, *96*, 78–87.
28. Vennes, I.; Mitri, H.; Chinnasane, D.R.; Yao, M. Large-scale destress blasting for seismicity control in hard rock mines: A case study. *Int. J. Min. Sci. Technol.* **2020**, *30*, 141–149. [CrossRef]
29. Andrieux, P.; Hadjigeorgiou, J. The destressability index methodology for the assessment of the likelihood of success of a large-scale confined destress blast in an underground mine pillar. *Int. J. Rock Mech. Min. Sci.* **2007**, *45*, 407–421. [CrossRef]
30. Fuławka, K.; Mertuszka, P.; Pytel, W.; Szumny, M.; Jones, T. Seismic evaluation of the destress blasting efficiency. *J. Rock Mech. Geotech. Eng.* **2022**, *14*, 1501–1513. [CrossRef]
31. Mertuszka, P.; Szumny, M.; Fuławka, K.; Kondoł, P. Novel approach for the destress blasting in hard rock underground copper mines. *J. Sustain. Min.* **2022**, *21*, 141–154. [CrossRef]
32. Lurka, A.; Stec, K. *Charakterystyka Radiacji Fal Sejsmicznych w Obszarze Epicentralnym dla Wstrząsów w LGOM, Warsztaty—Zagrożenia Naturalne w Górnictwie*; Wyższy Urząd Górniczy: Katowice, Poland, 2005. (In Polish)

33. Orlecka-Sikora, B.; Papadimitriou, E.E.; Kwiatek, G. A study of the interaction among mining induced seismic events in the Legnica-Glogow Copper District, Poland. *Acta Geophys.* **2009**, *57*, 2. [CrossRef]
34. Urban, P.; Wiejacz, P.; Domański, B. *Analiza Mechanizmów Wstrząsów Górniczych Występujących na Obszarze Legnicko-Głogowskiego Okręgu Miedziowego*; Geofizyka w Geologii i Górnictwie, wyd.; Wydział Nauk o Ziemi UŚ: Katowice, Poland, 2010. (In Polish)
35. Ren, F.Q.; Zhu, C.; He, M.; Shang, J.; Feng, G.; Bai, J. Characteristics and Precursor of Static and Dynamic Triggered Rockburst: Insight from Multifractal. *Rock Mech. Rock Eng.* **2023**, *56*, 1945–1967. [CrossRef]
36. Ren, F.; Zhu, C.; Yuan, Z.; Karakus, M.; Tang, S.; He, M. Recognition of shear and tension signals based on acoustic emission parameters and waveform using machine learning methods. *Int. J. Rock Mech. Min. Sci.* **2023**, *171*, 105578. [CrossRef]
37. Taylor, L.M.; Chen, E.P.; Kuszmaul, J.S. Microcrack-induced damage accumulation in brittle rock under dynamic loading. *Comput. Methods Appl. Mech. Eng.* **1986**, *55*, 301–320. [CrossRef]
38. Maxwell, S.C.; Young, R.P. Propagation effects of an underground excavation. *Tectonophysics* **1998**, *289*, 17–30. [CrossRef]
39. Chen, S.G.; Zhao, J. A study of UDEC modelling for blast wave propagation in jointed rock masses. *Int. J. Rock Mech. Min. Sci.* **1998**, *35*, 93–99. [CrossRef]
40. Ma, G.W.; Hao, H.; Zhou, Y.X. Modelling of wave propagation induced by underground explosion. *Comput. Geotech.* **1998**, *22*, 283–303. [CrossRef]
41. Zhu, Z.; Mohanty, B.; Xie, H. Numerical investigation of blasting-induced crack initiation and propagation in rocks. *Int. J. Rock Mech. Min. Sci.* **2007**, *44*, 412–424. [CrossRef]
42. Zhu, W.C.; Wei, C.H.; Li, S.; Wei, J.; Zhang, M.S. Numerical modeling on destress blasting in coal seam for enhancing gas drainage. *Int. J. Rock Mech. Min. Sci.* **2013**, *59*, 179–190. [CrossRef]
43. Ma, G.W.; An, X.M. Numerical simulation of blasting-induced rock fractures. *Int. J. Rock Mech. Min. Sci.* **2008**, *45*, 966–975. [CrossRef]
44. An, H.M.; Liu, H.Y.; Han, H.; Zheng, X.; Wang, X.G. Hybrid finite-discrete element modelling of dynamic fracture and resultant fragment casting and muck-piling by rock blast. *Comput. Geotech.* **2017**, *81*, 322–345. [CrossRef]
45. Baranowski, P.; Mazurkiewicz, Ł.; Małachowski, J.; Pytlik, M. Experimental testing and numerical simulations of blast-induced fracture of dolomite rock. *Meccanica* **2020**, *55*, 2337–2352. [CrossRef]
46. Tang, B.; Mitri, H. Numerical modelling of rock preconditioning by destress blasting. *Proc. Inst. Civ. Eng.-Ground Improv.* **2001**, *5*, 57–67. [CrossRef]
47. Baranowski, P.; Damaziak, K.; Mazurkiewicz, Ł.; Mertuszka, P.; Pytel, W.; Małachowski, J.; Pałac-Walko, B.; Jones, T. Destress Blasting of Rock Mass: Multiscale Modelling and Simulation. *Shock Vib.* **2019**, *2019*, 2878969. [CrossRef]
48. Xu, J.; Kang, Y.; Wang, X.; Feng, G.; Wang, Z. Dynamic characteristics and safety criterion of deep rock mine opening under blast loading. *Int. J. Rock Mech. Min. Sci.* **2019**, *119*, 156–167. [CrossRef]
49. Zheng, X.; Hua, J.; Zhang, N.; Feng, X.; Zhang, L. Simulation of the Load Evolution of an Anchoring System under a Blasting Impulse Load Using FLAC3D. *Shock Vib.* **2015**, *2015*, 972720. [CrossRef]
50. Sainoki, A.; Emad, M.Z.; Mitri, H.S. Study on the efficiency of destress blasting in deep mine drift development. *Can. Geotech. J.* **2017**, *54*, 518–528. [CrossRef]
51. Pytel, W.M.; Mertuszka, P.P.; Jones, T.; Paprocki, H. Numerical simulations of geomechanical state of rock mass prior to seismic events occurrence—Case study from a Polish copper mine aided by FEM 3D. In *Proceedings of the 27th International Symposium on Mine Planning and Equipment Selection*; Springer: Cham, Switzerland, 2019; pp. 417–427.
52. Yi, C.; Nordlund, E.; Zhang, P.; Warema, S.; Shirzadegan, S. Numerical modeling for a simulated rockburst experiment using LS-DYNA. *Undergr. Space* **2021**, *6*, 153–162. [CrossRef]
53. Vennes, I.; Mitri, H. Geomechanical effects of stress shadow created by large-scale destress blasting. *J. Rock Mech. Geotech. Eng.* **2017**, *9*, 1085–1093. [CrossRef]
54. Miao, S.; Konicek, P.; Peng-Zhi Pan, P.Z.; Mitri, M. Numerical modelling of destress blasting—A state-of-the-art review. *J. Sustain. Min.* **2022**, *21*, 278–297. [CrossRef]
55. Hoek, E.; Carranza-Torres, C.T.; Corkum, B. Hoeck-Brown failure criterion—2002 edition. In Proceedings of the NARMS-TAC Conference, Toronto, ON, Canada, 7–10 July 2002; Volume 1, pp. 267–273.
56. Pytel, W.; Mertuszka, P.; Fuławka, K.; Lurka, A.; Pałac-Walko, B. Resultant axial stresses in instrumented rockbolts induced by dynamic effects occurred due to multi-face blasting in the working areas. *Tunn. Undergr. Space Technol.* **2021**, *116*, 104088. [CrossRef]
57. Pytel, W.; Fuławka, K.; Pałac-Walko, B.; Mertuszka, P. Numerical and Analytical Determination of Rockburst Characteristics: Case Study from Polish Deep Copper Mine. *Appl. Sci.* **2023**, *13*, 11881. [CrossRef]
58. Kozłowska, M. Ilościowa analiza odległości epicentralnych wstrząsów względem frontu eksploatacji w O/ZG Rudna (LGOM). *Przegląd Górniczy* **2012**, *68*, 75–85. (In Polish)
59. Burtan, Z.; Zorychta, A.; Chlebowski, D.; Cieślik, J. Analiza sejsmiczności indukowanej w O/ZG „Rudna" w aspekcie rozmieszczenia ognisk wstrząsów względem frontu eksploatacyjnego. In Proceedings of the XXIII Międzynarodowa Konferencja Naukowo-Techniczna z Cyklu Górnicze Zagrożenia Naturalne, Szczyrk, Poland, 8–10 November 2016. (In Polish).

Disclaimer/Publisher's Note: The statements, opinions and data contained in all publications are solely those of the individual author(s) and contributor(s) and not of MDPI and/or the editor(s). MDPI and/or the editor(s) disclaim responsibility for any injury to people or property resulting from any ideas, methods, instructions or products referred to in the content.